2021 Joint International EUROSOI Workshop and International Conference on Ultimate Integration on Silicon (EuroSOI-ULIS) | 978-1-6654-3745-5/21/$31.00 ©2021 IEEE | DOI: 10.1109/EuroSOI-ULIS53016.2021.9560173

# Conductance due to the Edge Modes in Nanoribbons of 2D Materials in a Topological Phase

Viktor Sverdlov
*Christian Doppler Laboratory for Nonvolatile Magnetoresistive Memory and Logic at the Insitute for Microelectronics, Technische Universität Wien*
Vienna, Austria
sverdlov@iue.tuwien.ac.at

Heribert Seiler
*Institute for Microelectronics Technische Universität Wien*
Vienna, Austria
seiler@iue.tuwien.ac.at

Al-Motasem Bellah El-Sayed
*Institute for Microelectronics Technische Universität Wien*
Vienna, Austria and
*Nanolayers Research Computing Ltd. 1 Granville Court London, U.K.*
el-sayed@iue.tuwien.ac.at

Hans Kosina
*Institute for Microelectronics Technische Universität Wien*
Vienna, Austria
kosina@iue.tuwien.ac.at

***Abstract*—Employing novel 2D materials with topologically protected current-carrying edge states is promising to boost the on-current in electronic devices. Using nanoribbons is essential to reduce the contribution of the 2D bulk states to the current. Making the nanoribbon widths narrower allows one to put more current-carrying edge states under the gate of a fixed width thus boosting the current. However, the edge states start to interact in narrow nanoribbons. Based on an effective k·p model, we analyze the topologically protected edge states and their conductance for several 2D materials as a function of the normal electric field. We compare the 2D materials $MoS_2$, $MoSe_2$, $WS_2$, and $WSe_2$ in the topological 1T′ phase and find the largest electric field-induced conductance modulation is in $MoS_2$ nanoribbons.**

***Keywords—Topologically Protected Edge States; Topological Insulators; Nanoribbons; k·p Method; Conductance.***

## I. Introduction

The use of novel materials with advanced properties is mandatory to continue with the device scaling for high performance applications at reduced power. Topological insulators (TIs) belong to a new class of materials possessing highly conductive edge states with a nearly linear dispersion lying in the band gap. These states are topologically protected and therefore immune to backscattering. If the Fermi level lies in the gap, the large on-current is carried by the highly conductive edge states. Applying a gate voltage allows one to move the Fermi level in the conduction or the valence bands. It prompts strong scattering between the edge and the bulk electron or hole states [1]. This leads to a substantial reduction of the current, resulting in an on/off current ratio suitable for device applications [1].

Recently, it was predicted that well-known monolayer-thin two-dimensional (2D) materials with high promise for future microelectronic devices [2] can also be found in a 1T′ TI phase [3]. The band gap within which the edge states exist is opened by the spin-orbit interaction at the intersections (degeneracy points) between the inverted electron and hole bands. The value of the gap can be modulated by an external electric field $E_z$ normal to the 2D sheet. The band gap in the inverted band structure is reduced and can be completely closed upon increasing values of $E_z$. By further increasing $E_z$ the band gap reopens again; however, the traditional electron and hole band order is restored indicating a topological phase transition from a non-trivial topological to a trivial insulator. In contrast to the TI phase where the highly conductive edge states carry a large current if the in-plane field is applied, no current-carrying edge states are allowed in the trivial insulating phase. Therefore, there is no current due to the edge states. The electric field induced topological phase transition between the TI and the trivial insulating phases peculiarities of the band structure in topological phases offers an alternative way to modulate the current by the gate voltage and to design the current switches.

To enhance the on-current density due to the edge states it is mandatory to have many edges. One can achieve this by placing several nanoribbons under the gate. The narrower the nanoribbon is, the more nanoribbons one can assemble within a given gate width. At the same time, the contribution due to the 2D bulk states decreases with shrinking width [4].

However, the behaviour of the edge states in a narrow nanoribbon is different from that at the edge of an infinite 2D sheet. Indeed, a small gap in the gapless spectrum of the edge states opens due to an interaction of the topologically protected states from the opposite edges [5,6]. Because of this gap in the dispersion of the edge modes, their conductance is found to be slightly less than the ideal conductance $G_0 = 2e^2/h$.

This gap between the edge states initially increases with increasing normal field $E_z$ until the edge modes' dispersion meets the 2D bulk conduction and valence bands. Their conductance decreases accordingly. It was argued [6] that after the edge modes dispersions as a function of the normal electric field meet the 2D bulk conduction and the valence band, they become indistinguishable from bulk bands. As the fundamental gap in TI decreases with $E_z$, the gap in the edge states spectrum shrinks and becomes zero, following the bulk dispersion [6]. Therefore, according to [6], the ballistic conductance due to the edge states increases and reaches the ideal value $G_0 = 2e^2/h$ at the critical electric field $E_0$ when the gap between the electron and hole bands closes. At even larger $E_z > E_0$ the bulk gap opens again signifying a transition to a trivial dielectric. However, the topological edge states are not allowed, and the conductance abruptly drops to zero [6] due to the phase transition from the TI to the trivial insulator state. This discontinuous behaviour of the ballistic conductance is unphysical. Considering a 1T′ $MoS_2$ nanoribbon as an example, we demonstrated in [7] that the erroneous results [6] were due to the spurious solutions of the dispersion equation. If the spurious solutions are disregarded, a qualitatively different behavior of the ballistic conductance in a 1T′ $MoS_2$ nanoribbon is obtained [7]. Namely, it was

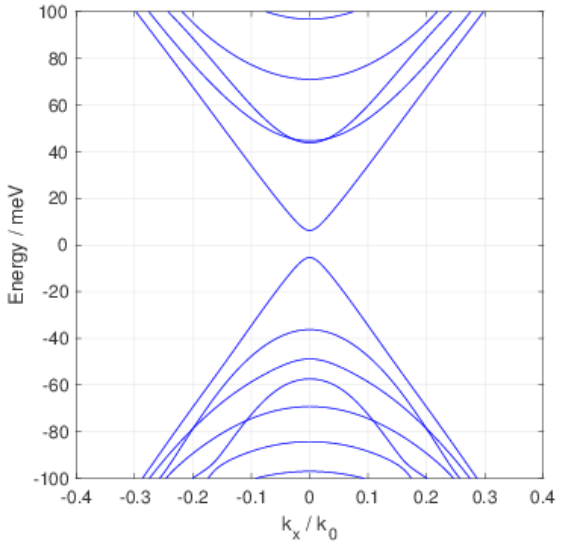


Fig.1 *S*ubband structure in a $MoS_2$ nanoribbon of width $d$=20nm at $E_z = 0$. The subbands with the linear dispersion and a small gap at $k_x = 0$ correspond to the edge modes.

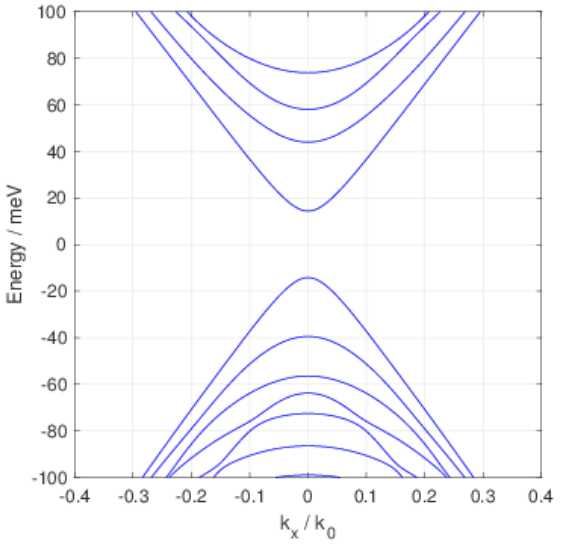


Fig.2 *S*ubband structure in a $MoS_2$ nanoribbon of width $d$=20nm at the critical field $E_z = \alpha^{-1}\nu_2$ at which the spin-orbit gap in the 2D sheet closes. In contrast, the gap in the nanoribbon increases.

demonstrated that the gap between the edge modes always increases with the field $E_z$ and, in contrast to [6], never closes. The increase in the separations between the electron and hole subbands results in a continuous and substantial decrease in the edge channels ballistic conductance.

In this work we evaluate the edge states and their corresponding Landauer conductance in a nanoribbon in the 1T′ TI phase. In addition to $MoS_2$ we consider potentially relevant 2D materials $MoSe_2$, $WS_2$, and $WSe_2$.

## II. Method

The subbands in a nanoribbon of a topological 2D material are found by solving the Schrödinger equation with the effective Hamiltonian $H$ [7]:

$$\boldsymbol{H} = \begin{pmatrix} H(\mathbf{k}) & 0 \\ 0 & H^{+}(-\mathbf{k}) \end{pmatrix}, \qquad (1)$$

$$H(\boldsymbol{k}) = \begin{pmatrix} \frac{1}{2} - k_y^2\frac{m}{m_y^p} - k_x^2\frac{m}{m_x^p} + U(\mathrm{y}) & v_2 k_y - \alpha E_z + i v_1 k_x \\ v_2 k_y - \alpha E_z - i v_1 k_x & \frac{-1}{2} + k_y^2\frac{m}{m_y^d} + k_x^2\frac{m}{m_x^d} + U(\mathrm{y}) \end{pmatrix} \qquad (2)$$

| Variable | $MoS_2$ | $MoSe_2$ | $WS_2$ | $WSe_2$ |
|---|---|---|---|---|
| δ [eV] | 0.55 | 0.76 | 0.17 | 0.69 |
| $\boldsymbol{v_1}$[m/s] | 3.38 $10^5$ | 3.42 $10^5$ | 2.93 $10^5$ | 3.54 $10^5$ |
| $\boldsymbol{v_2}$ | 0.23 $10^5$ | 0.23 $10^5$ | 0.85 $10^5$ | 0.38 $10^5$ |
| $\boldsymbol{m_x^p/m_e}$ | 0.48 | 0.28 | 0.53 | 0.36 |
| $\boldsymbol{m_y^p/m_e}$ | 0.29 | 0.17 | 0.28 | 0.16 |
| $\boldsymbol{m_x^d/m_e}$ | 2.32 | 2.65 | 3.2 | 3.28 |
| $\boldsymbol{m_y^d/m_e}$ | 0.92 | 3.14 | 8.2 | 8.4 |
| $\boldsymbol{\alpha/e}$ [nm] | 0.016 | 0.027 | 0.017 | 0.024 |
| $\boldsymbol{k_0}$ [$nm^{-1}$] | 1.8 | 1.9 | 1.08 | 1.7 |

Table I Parameters [6] used in the model. $m_e$ is the electron mass, $e$ is the electron charge.

Here $U(\mathrm{y})$ is the confinement potential. For convenience we introduced the dimensionless units by measuring all energies in units of the separation $\delta$ between the electron and hole bulk bands at the Γ-point in the inverted band structure, while the wave vectors $k = (k_x, k_y)$ are in units $k_0 = \frac{2\delta}{\hbar^2}\frac{m_y^d m_y^p}{m_y^d + m_y^p}^{1/2}$, where $m_{y(x)}^{d(p)}$ are the effective masses, $m = \frac{m_y^d m_y^p}{m_y^d + m_y^p}$ and $\nu_{1(2)}$ are the velocities characterizing the strength of the spin-orbit interaction. The parameters used in simulations as well as the values of $k_0$ are given in Table I.

The block-diagonal form of (1) simplifies the solution for the subbands as the solution of the lower block is the time-reversal solution [5,7] of the upper block. It is therefore sufficient to solve the Schrödinger equation with (2). If the nanoribbon is cleaved along the *OX* axis and the confinement potential is approximated by an infinite square well of the

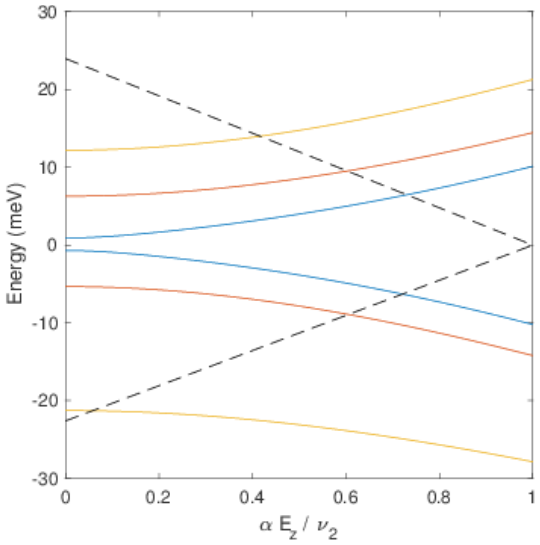


Fig.3 Energies of the electron and hole edge states in a $MoS_2$ nanoribbon of the width $d$=30nm (blue), $d$=20nm (orange) and $d$=10nm (yellow) as a function of electric field strength. Dashed line: bulk bands extrema.

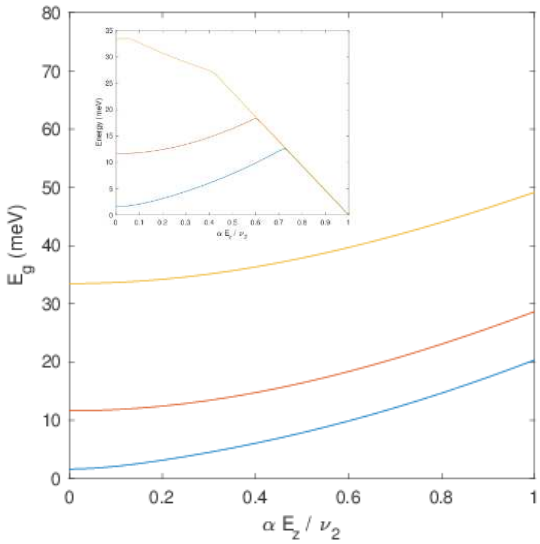


Fig.4 Energy gap in the edge states spectrum in a $MoS_2$ nanoribbon of the width $d$=30nm (blue), $d$=20nm (orange) and $d$=10nm (yellow). Inset: energy separation including the bulk bands extrema shown by dashed line in Fig.3

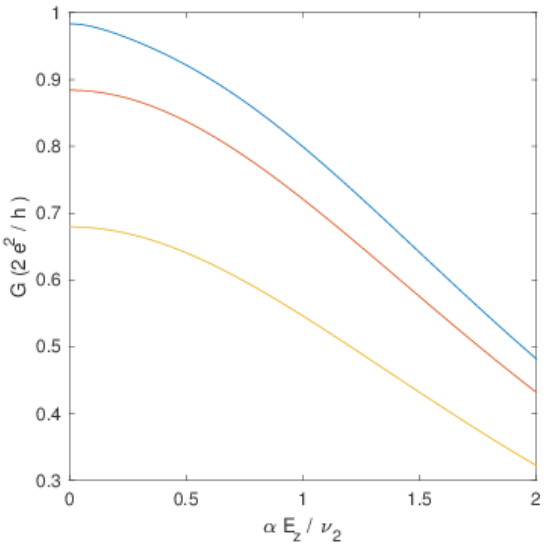


Fig.5 Ballistic conductance due to the lowest electron and topmost hole edge states for a $MoS_2$ nanoribbon of the width $d$=30nm (blue), $d$=20nm (orange) and $d$=10nm (yellow).

width $d$, the eigenfunction of the upper block in (1) satisfies the boundary conditions

$$\psi_{k_x}(y = \pm d/2) = 0. \quad (3)$$

The wave functions and the edge modes dispersion relations are found numerically using the Newton method [7]. While solving the corresponding dispersion equation, special care must be taken to avoid spurious solutions [7] which lead to erroneous results and unphysical interpretations.

## III. Results

Fig.1 shows the subband structure obtained with the Hamiltonian (1,2) and the boundary condition (3) in a 20nm wide 1T′ $MoS_2$ cleaved along the $OX$ axis, at $k_x = 0$ and in the absence of the normal electric field ($E_z = 0$). The energies are offset by $\Delta E = \frac{1}{2}\frac{m_y^d - m_y^p}{m_y^d + m_y^p}$ for convenience. Fig.2 demonstrates the subbands at the electric field $E_z = \alpha^{-1}\nu_2$. This value of the field is critical for the band structure in an infinite sheet of a 2D material. Indeed, at this electric field value the fundamental gap closes. With a further increase of the normal field the gap opens again; however, the material becomes a trivial dielectric, without topologically protected edge states.

In a nanoribbon, however, the subband spectrum remains gapped at the critical electric $E_z = \alpha^{-1}\nu_2$. Furthermore, the gap between the lowest electron-like and the top-most hole-like subbands seems to increase with the field. To confirm this observation, the dependence of the minimum of the lowest electron-like and the maximum of the topmost hole-like subbands as a function of the normal electric field is shown in Fig.3, for three different nanoribbon widths of 10 nm, 20 nm, and 30 nm. We observe that the gap between the subbands is larger for narrower nanoribbons. At the same time, the gap increases as a function of the field, for all three widths as shown in Fig.4. This contrasts with the dependence of the fundamental band gap in an infinite 2D sheet shown by dashed lines in Fig.3. The 2D bulk band gap decreases with the normal field and becomes zero as expected at the critical value of $E_z = \alpha^{-1}\nu_2$ at the electric field.

In a 2D sheet the TI - trivial insulator phase transition happens exactly at the critical value of the normal field. If the behavior of the fundamental gap in the 2D bulk is opposite to that of the subbands in a nanoribbon, the question arises how the phase transition between the TI and a trivial insulator appears in a nanoribbon. It turns out that if the energies of the subbands are within the bulk band gap at small values of $E_z$, the envelope wave functions are localized at opposite edges of the nanoribbon [7]. When the subbands' dispersions approach the dashed line in Fig.3 corresponding to the 2D bulk bands, the localization becomes weaker and disappears completely at the points of crossing. The transition appears earlier in narrower nanoribbons. With the field further increased, the subbands, however, do not align themselves with the bulk bands, claimed in [6]. Instead, their energies evolve to the bulk conduction and valence bands. Therefore, the nature of the

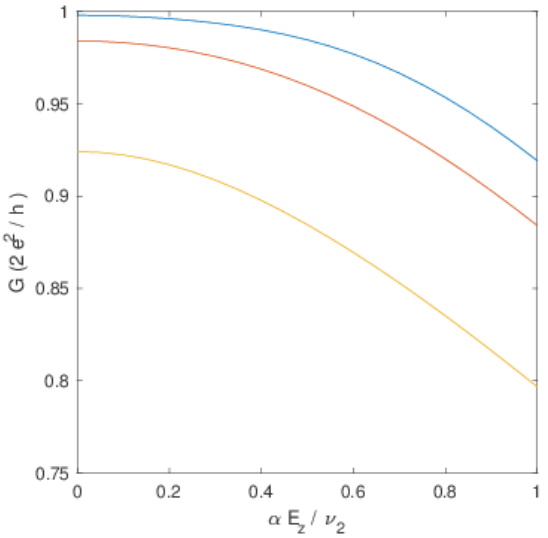


Fig.6 Ballistic conductance due to the lowest electron and topmost hole edge states for a $MoSe_2$ nanoribbon of the width d=30nm (blue), $d$=20nm (orange) and $d$=10nm (yellow).

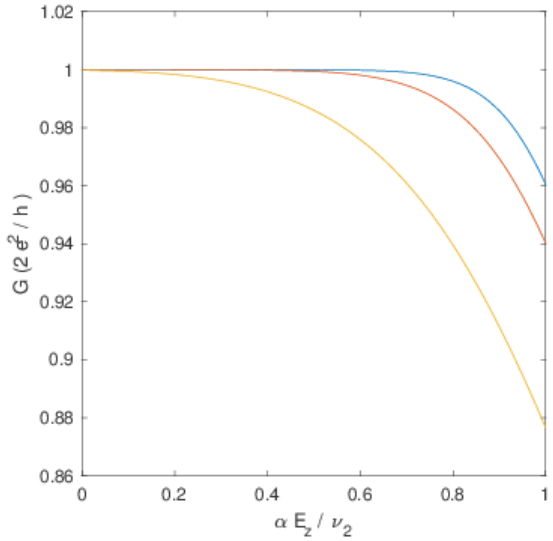


Fig.7 Same as in Fig.6 for $WS_2$ nanoribbons.

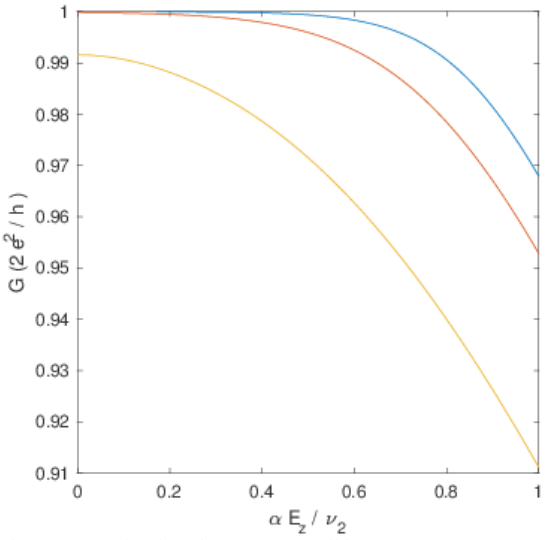


Fig.8 Same as in Fig.6 for $WSe_2$ nanoribbons.

envelope function in the direction normal to the nanoribbon changes from the one localized at the edges to a nonlocalized bulk-like behavior. We can therefore assign a TI to a trivial insulator phase transition in a confined geometry to the change of the wave function behavior appearing precisely at the points of the intersections of the bulk 2D bands with the subbands' dispersions (Fig.3). This transition happens at larger normal fields in broader nanoribbons thus recovering the TI to trivial insulator phase transition in a 2D geometry.

Fig.4 shows that the separation between the lowest electron-like and topmost hole-like subbands, according to Fig.3, increases with $E_z$ and is largest for the 10 nm nanoribbon. If, however, the 2D bulk bands shown in Fig.3 with dashed lines were also included, the separations shown in Fig.4 would look like those in the inset of Fig.4. This is precisely the behavior shown in Fig.5a of the reference [6]. That behavior is not correct, however, as it is caused by spurious solutions of the dispersion equation. As we demonstrated in [7], these spurious solutions coincide with the dispersion of the bulk 2D bands. As they do not depend on the nanoribbon width $d$, they must be neglected and do not contribute to the ballistic conductance.

Finally, following [6], we evaluate the ballistic conductance due to the lowest electron-like and topmost hole-like subbands as a function of the normal electric field for the nanoribbon made of $MoS_2$, $MoSe_2$, $WS_2$, and $WSe_2$ materials in 1T′ topological phase, with the corresponding parameters listed in Table I. To exploit the Landauer expression for the conductance we need the subbands' dependence on the field shown in Fig.3 but evaluated for all materials. It is assumed that the chemical potential is at zero energy while the temperature is 300 K. Fig.5 shows the ballistic conductance due to the above described subbands. The conductance decreases with the electric field for all nanoribbons' widths including the one of 10 nm. This is in contrast to the behavior predicted in [6] where the conductance of a 10 nm thin nanoribbon is predicted to increase with the normal electric field. As explained, this erroneous behavior of the conductance is due to the spurious solutions of the dispersion equation. The dependence of the corresponding ballistic conductance in $MoSe_2$, $WS_2$, and $WSe_2$ nanoribbons is shown in Fig.6, Fig.7, and Fig.8, correspondingly. As the separation between the lowest electron-like and topmost hole-like subbands increases with the field, the ballistic conductance decreases. However, the largest conductance modulation is found in $MoS_2$ nanoribbons.

## IV. Conclusion

A **k·p** method is applied to investigate the topologically protected states at the edges of nanoribbons of several 2D materials as a function of the normal electric field. It is demonstrated that the electric field-induced conductance modulation is largest in 1T′ $MoS_2$ nanoribbons making them more suitable candidates for use in ultra-scaled devices.

## Acknowledgment

Financial support by the Austrian Federal Ministry for Digital and Economic Affairs and the National Foundation for Research, Technology and Development and the Christian Doppler Research Association is gratefully acknowledged.

## References

[1] W.G.Vandenberghe and M. V. Fischetti, "Imperfect two-dimensional topological insulator field-effect transistors", Nature Communications, vol.8, art.14184 (pp. 1-8), 2017. doi: 10.1038/ncomms14184

[2] Yu.Yu. Illarionov, A.G. Banshchikov, D.K. Polyushkin, S. Wachter, T. Knobloch, M. Thesberg, L. Mennel, M. Paur, M. Stöger-Pollach, A. Steiger-Thirsfeld, M.I. Vexler, M. Waltl, N.S. Sokolov, T. Mueller, and T. Grasser, "Ultrathin calcium fluoride insulators for two-dimensional field-effect transistors", Nature Electronics, vol.2, pp.230-235, 2019. doi: 10.1038/s41928-019-0256-8

[3] X. Qian, J. Liu, L. Fu, and Ju Li., "Quantum spin Hall effect in two-dimensional transition metal dichalcogenides", Science, vol. 346, issue 6215, pp.1344-1347, 2014. doi: 10.1126/science.1256815

[4] M.J. Gilbert, "Topological electronics" Communications Physics, vol. 4, art.70 (pp.1-12), 2021. oi: 10.1038/s42005-021-00569-5

[5] B. Zhou, H.-Z. Lu, R.-L. Chu, S.-Q. Shen, and Q. Niu, "Finite size effects on helical edge states in a quantum spin-Hall system" Phys.Rev.Lett., vol.101, art.246807 (pp.1-4), 2008. doi: 10.1103/PhysRevLett.101.246807

[6] B. Das, D. Sen, S. Mahapatra, "Tuneable quantum spin Hall states in confined 1T' transition metaldichalcogenides," Scientific Reports, vol. 10 (2020), art. 6670. doi: 10.1038/s41598-020-63450-5

[7] V. Sverdlov, A.-M. El-Sayed, H. Seiler, H. Kosina, and S. Selberher. "Subbands in a Nanoribbon of Topologically Insulating $MoS_2$ in the 1T′ Phase", Solid-State Electron., vol. 184, art. 108081 (pp.1 – 9), 2021. doi:10.1016/j.sse.2021.108081